**Advances in Nano Research**, *Vol. 19, No. 2 (2025) 117-127*
https://doi.org/10.12989/anr.2025.19.2.117


# Investigation of the effect of changes in material values of FSPed Al5754 on contact mechanics

Dursun Murat Sekban[1,2], Semih Mahmut Aktarer[3], Mehmet Emin Özdemir[4], Ecren Uzun Yaylacı[5], Ahmet Emre Pirim[6], Reza Kolahchi[7] and Murat Yaylacı[*6,8,9]

[1]*Department of Marine Engineering Operations*, *Karadeniz Technical University*, *61080*, *Trabzon*, *Turkey*
[2]*WMS Engineering Services Industry Trade Limited Company*, *61080*, *Trabzon*, *Turkey*
[3]*Department of Automotive Technology*, *Recep Tayyip Erdogan University*, *53020*, *Rize*, *Turkey*
[4]*Department of Civil Engineering*, *Cankiri Karatekin University*, *18100*, *Çankırı*, *Turkey*
[5]*Faculty of Fisheries*, *Recep Tayyip Erdogan University*, *53100*, *Rize*, *Turkey*
[6]*Turgut Kıran Maritime Faculty*, *Recep Tayyip Erdogan University*, *53900*, *Rize*, *Turkey*
[7]*Department of Civil Engineering*, *Islamic Azad University*, *Jasb*, *Iran*
[8]*Department of Civil Engineering*, *Recep Tayyip Erdogan University*, *53100*, *Rize*, *Turkey*
[9]*Murat Yaylacı-Luzeri R&D Engineering Company*, *53100*, *Rize*, *Turkey*

(*Received April 23, 2025, Revised July 30, 2025, Accepted July 31, 2025*)

**Abstract.** The friction stir process (FSP), which is widely used on plate-type materials, was applied to AA5754 alloy, commonly used in engineering applications, under three different parameter settings. The effects of this process on the strength and elongation values were then evaluated. In the next stage, the material properties of the contact problem were designed using finite element-based (FEM) modeling techniques, and the effects of the changes in the strength and elongation values of the material on the contact stress and distance were determined. As a result of the examinations, it was determined that in all the changing parameters, the strength values increased compared to the initial state of the material after FSP. The elongation values may decrease or increase depending on the specific FSP parameters used. Regarding the contact stress and contact distance values, it was determined that the contact stress values increased in direct proportion to the strength of the material. It was determined that the changes in the elongation values of the material were more effective in the change of contact distances.
**Keywords:** Al5754; contact mechanics; finite element analysis; friction stir process

## 1. Introduction

Aluminum alloys are commonly used in many engineering applications because of their low weight, ease of machining, and strong corrosion resistance. While a variety of aluminum alloys are employed in engineering, it is known that AA5754 alloy is often preferred, especially for its high strength, good formability, and excellent corrosion resistance (Das *et al*. 2020).

As is known, parts used in engineering applications are often used in contact with each other. It is also highly critical to understand the contact pressure and contact areas that occur at the time of contact to prevent any issues in case of contact problems. It is well known that the material's strength and ductility significantly influence both the contact pressure and contact area during loading (Öner 2021a, b, Öner and Birinci 2014, 2020). However, it is also known that the studies carried out to reveal the effects of the changes in strength and elongation in materials on structures in contact are extremely limited (Pointner 2008, Ghaednia *et al*. 2017). Recent research has shown that contact mechanics, which involves the direct interaction of surface asperities, plays a vital role in local deformation, frictional response, and wear development at metallic interfaces (Ammarullah *et al*. 2025). Simultaneously, new research using computational and experimental methods, such as discrete element modeling, has emphasized the significance of material behavior under complex loading and contact conditions (Fu *et al*. 2025a, b, Haeri and Sarfarazi 2016, Sarfarazi *et al*. 2017).

It is possible to divide the methods that can be applied to simultaneously change the strength and elongation values of materials into two: heat treatments and severe plastic deformation (SPD) methods. SPD methods are advantageous over heat treatments in terms of their effect on mechanical properties. On the other hand, among the SPD methods, the friction stir process (FSP) stands out in terms of its applicability to various material types, including plate-type materials (Mishra *et al*. 2014, Leal *et al*. 2015, Aktarer *et al*. 2017, Padhy *et al*. 2018, Wang *et al*. 2020, Singh *et al*. 2023, Sekban 2024). It is known from the literature that FSP has significant effects on the strength and elongation values of various material groups (Starink *et al*. 2008, Surekha and Els-Botes 2011, Guru *et al*. 2015, Khodabakhshi *et al*. 2017, Kumar *et al*. 2017, Chaudhary *et al*. 2018, Yang *et al*. 2024). When these effects were examined, it was determined that strength values generally improved and elongation values decreased as a result of grain refinement after FSP (Yadav and Bauri 2012, Sekban *et al*. 2015,

*Corresponding author, Professor
E-mail: murat.yaylaci@erdogan.edu.tr



ISSN: 2287-237X (Print), 2287-2388 (Online)

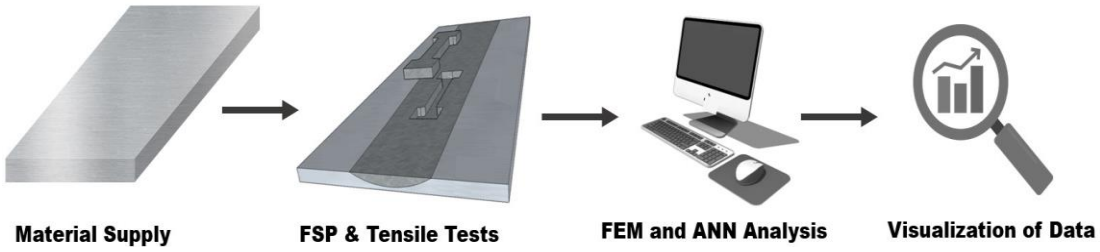


Fig. 1 Schematic representation of the working flow

Table 1 Parameter codes and FSP parameters used in the study

| Parameter Code | Feed Rate (mm/min) | Rotational Speed (rpm) | Tool Pressure (kg) |
|---|---|---|---|
| FSPed P1 | 115 | 1250 | 700 |
| FSPed P2 | 210 | 1250 | 700 |
| FSPed P3 | 400 | 1250 | 700 |

Aktarer *et al*. 2019, Singh *et al*. 2020). On the other hand, the literature indicates that the parameters used during FSP are highly effective in obtaining the mechanical properties (Surekha *et al*. 2009, Karthikeyan and Senthil Kumar 2011, Vaira Vignesh and Padmanaban 2018, Abrahams *et al*. 2019, Zhao *et al*. 2019).

Although it is applied to many different material groups, studies on the application of FSP to Al5754 alloy are minimal (Serio *et al*. 2016, Tosun *et al*. 2020). On the other hand, a study examining the effects of changes in the strength and elongation values of the FSPed Al 5754 alloy on contact pressure and contact areas has not been conducted yet. In this study, FSP was applied to Al 5754 alloy in three changing parameters, and the changes in the strength and elongation values of the material after FSP were examined in comparison with the situation before the process. In the next phase of the study, the changing strength and elongation values were transferred to finite element (FEM) analysis to reveal the effects of these changes on the contact stresses and distance values of the structures in contact. As a result of the examinations, the strength values of Al 5754 increased in all parameters after FSP. The elongation values could be higher or lower than the main structure according to the changing parameters. As a result of FEM analysis, it was determined that contact stresses increased with the strength of the material in all changing input parameters, such as external load, circular punch radius, and quarter plane spacing distance, and the changing elongation values of the materials were more effective on the contact distances. Although friction stir processing (FSP) has been extensively studied for various aluminum alloys (El-Sayed *et al*. 2025, Naumov *et al*. 2025, Wang *et al*. 2025), its specific influence on contact mechanics—especially regarding the modification of mechanical properties like strength and elongation—has not been thoroughly explored for the AA5754 alloy. This research fills that gap by analyzing how changes in these properties, caused by different FSP parameters, impact contact stresses and contact distances within a two-body contact model based on finite element analysis. The goal is to offer insights into how mechanical improvements from FSP can be intentionally used to enhance contact performance, particularly in surface-focused mechanical systems where factors such as contact pressure distribution, wear resistance, and stress concentration are crucial.

## 2. Experimental procedure

### *2.1 Material and FSP*

In the study, a 6 mm thick AA 5754 alloy, which is commonly used in the automotive, aviation, construction, and marine industries, was used. After tensile tests determined the strength and elongation values of the material subjected to FSP with three varying parameters, the effects of these changing material properties on contact pressure and areas were comparatively examined through FEM analyses. The working systematics is shown schematically in Fig. 1.

FSP processes were applied to the material used in the study at three different feed rates (115 mm/min, 210 mm/min, and 400 mm/min) and a rotational speed of 1250 rpm, as shown in Table 1. During FSP, a mixer set made of WC material with a length of 5.7 mm, a pin diameter of 8 mm, and a shoulder diameter of 16 mm was used. The tool inclination angle was determined as 30, and a constant tool pressure load of 700 kg was selected as the tool pressing force.

To determine the changes in strength and elongation values of the material after FSP, tensile tests were carried out at room temperature using an Instron 3382 brand device. The force-elongation values measured during the test were transferred to the computer, and stress-strain curves were drawn. The samples used in the tests were cut in 1.4 mm × 3 mm × 8 mm dimensions using a wire erosion cutting device, in the direction of FSP, within the area where FSP was applied, as seen in Fig. 2. For each case, at least three samples were tested and the averages of the values obtained were included in the study.

### *2.2 Finite element analysis*

The finite element method is advantageous for examining the behavior of theoretical designs under specified boundary conditions before experimental studies (Güvercin *et al*. 2025, Yemenoglu *et al*. 2025, YayIacı *et al*. 2025, Öner *et al*. 2025, Wu 2023, Wang *et al*. 2023, Turan *et al*. 2025). In addition to its flexibility in modeling complex geometries,

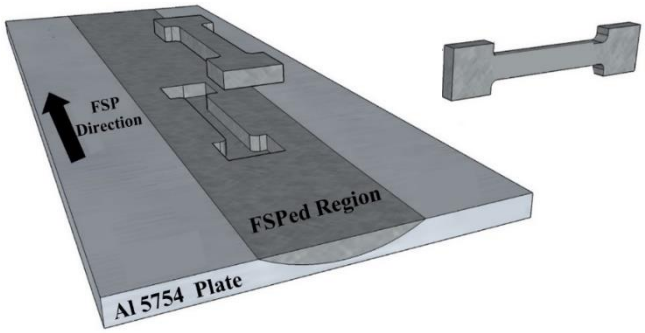


Fig. 2 Schematic representation of the FSP and tensile test specimen

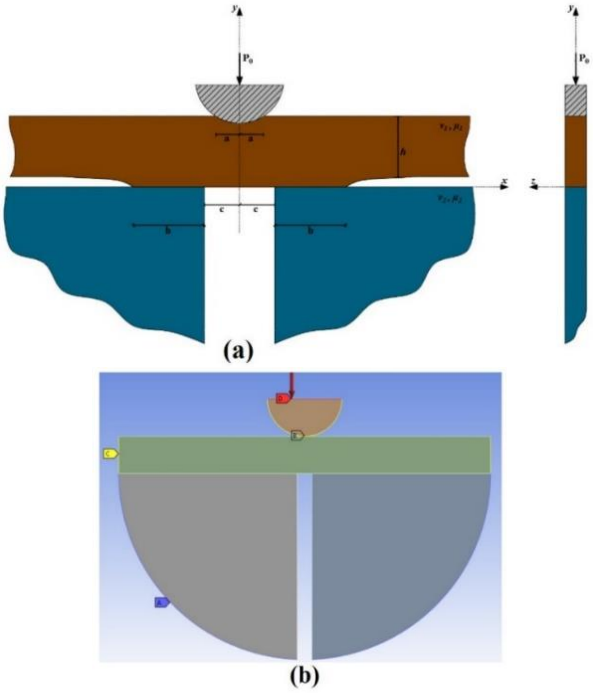


Fig. 3 (a) Contact problem geometry and (b) 2D analysis model

Table 1 Parameter codes and FSP parameters used in the study

| Parameter Code | Feed Rate (mm/min) | Rotational Speed (rpm) | Tool Pressure (kg) |
|---|---|---|---|
| FSPed P1 | 115 | 1250 | 700 |
| FSPed P2 | 210 | 1250 | 700 |
| FSPed P3 | 400 | 1250 | 700 |

FEM offers significant advantages in terms of reduced experimental cost and time efficiency compared to full-scale testing and analytical solutions (Ammarullah 2025, Hidayat *et al*. 2024). It minimizes the material burden arising from experimental studies and prevents the loss of time by allowing the change and application of different boundary conditions in a short time. In the finite element method, the analysis model is divided into a finite number of small parts, the behavior of these elements during loading is calculated, and the model's behavior is determined. Since the finite number of parts called elements shows the same mechanical properties as the model in every region, the simulation gives realistic results (Kiarasi *et al*. 2021, El-Ashmawy and Xu 2022, Zheng 2022, Moulgada *et al*. 2024, Benouis *et al*. 2024, Fuyad *et al*. 2024, Sekban *et al*. 2024a, b, Selvamani *et al*. 2024). The key steps for analysis—like modifying loadings in the model, changing materials, and reviewing various result parameters—are straightforward to organize. The chosen FEM model was selected for this study because of its proven reliability and efficiency in simulating contact problems with varying material properties. Its capacity to quickly incorporate different boundary conditions and material inputs makes it well-suited for evaluating the mechanical effects of friction stir processing within contact mechanics models.

This study section performed a finite element analysis of the contact problem in Fig. 3a using the ANSYS Workbench program.

First, a two-dimensional model of the contact problem compatible with mathematical reality was created (Fig. 3b). The mesh strategy was guided by convergence accuracy and stability considerations, which are congruent with known techniques in recent contact-based FEM investigations (Muchammad *et al*. 2024, Murugesan *et al*. 2025). Then, the model was divided into a finite number of pieces, and the mesh structure was formed. The mesh structure was generated using the 2D triangular-PLANE183 element, which is useful for creating finite element models with various geometric properties and yields remarkable results in plane-strain analyses. The mesh structure of the contact region was constructed with TARGE169 and CONTA172 elements that are quite compatible with each other. The mesh structure created under the specified boundary conditions comprises 15892 elements and 32564 nodes (Fig. 4a).

In the contact problem, the elastic layer sits on two elastic quarter planes, and it is loaded with a rigid punch. In the FEM model, all materials were assumed to be homogeneous, isotropic, and linearly elastic, which is a common and effective simplification in contact mechanics studies for metals (Lamura *et al*. 2024). The thickness of the elastic layer is determined as h = 100 mm, and its length is L = 1000 mm. As can be understood from the problem, there are two contact regions. The first is the elastic layer with a rigid punch, and the second is the elastic layer with a quarter plane. All contacts are assumed to be frictionless, and the effect of gravity is neglected. Thermal effects were neglected, and the simulations were carried out under isothermal conditions, as also done in previous similar studies (Tauviqirrahman *et al*. 2024). The problem is solved as a plane strain problem. The stress distribution obtained from the analysis and the images of the stresses occurring in the contact regions are given in Figs. 4b and 4c.

## 3. Results and discussions

### *3.1 Strength and elongation*

The stress-strain curve of the initial state of the material and after FSP was applied to 3 different parameters is shown in Fig. 5. Additionally, the strength and elongation

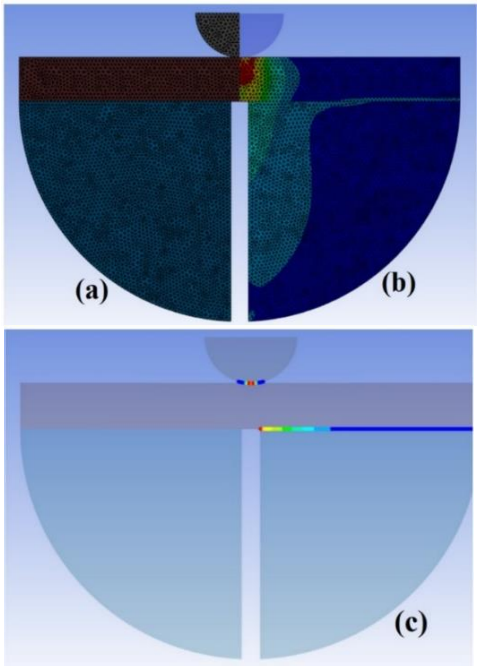


Fig. 4 (a) Mesh structure, (b) general stress distribution obtained as a result of the analysis, and (c) stress distribution in contact regions

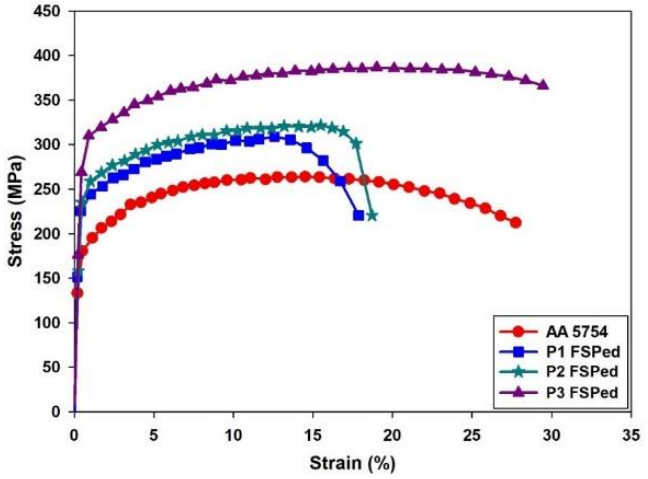


Fig. 5 (a) Stress-strain curves of samples before and after FSP

Table 2 Strength and elongation values before and after FSP

| Condition | Yield Strength (MPa) | Tensile Strength (MPa) | Uniform Elongation (%) | Total Elongation (%) |
|---|---|---|---|---|
| AA 5754 | 168±04 | 261±07 | 14.7±0.5 | 27.4±1.3 |
| P1 FSPed | 235±09 | 314±08 | 12±0.7 | 17.6±1.1 |
| P2 FSPed | 244±13 | 327±12 | 13.8±0.8 | 18.4±1.1 |
| P3 FSPed | 291±11 | 378±13 | 21.2±1.4 | 29.2±1.5 |

values obtained from this curve are shown in Table 2. As can be seen, the yield and tensile strength values of the main structure, which are 168 MPa and 261 MPa, respectively, increased to 235 MPa and 314 MPa after FSP in the parameters coded as P1, 244 MPa and 327 MPa after FSP in the parameters coded as P2, and 291 MPa and 378 MPa after FSP in the parameters coded as P3. In the literature, it is seen that there is a similar increase in strength values after FSP is applied to similar materials (Aktarer *et al*. 2017, Sun *et al*. 2019). Dynamic recrystallization occurring during FSP causes thinning in the grain structure, which causes an increase in strength values. However, it was observed that the elongation values of the main structure (uniform elongation: 14.7% and total elongation: 27.4%) decreased after FSP in P1 and P2 parameters. On the other hand, after the FSP was performed on the P3 parameter, both the uniform elongation and total elongation values compared to the main structure increased to 21.2% and 29.2%, respectively. The decrease in elongation values after FSP is generally explained by the limited dislocation movement following the thinning in the grain structure (Sekban 2024, Sekban *et al*. 2024b). Also, it is stated in the literature that the increase in elongation values in similar aluminum alloys after FSP is related to the refining and more uniform distribution of some phases in the alloy after FSP (WP 5).

These findings indicate that FSP can be used not only to increase the strength of AA5754 but also to adjust its ductility by modifying process parameters. This is especially beneficial in applications that require both formability and high contact performance, such as automotive structural panels or marine components.

### *3.2 Contact mechanism*

The numerical solution input dataset consists of three different parameters. These are as follows:

P: External load

R: Circular punch radius

c: Quarter plane spacing distance

The output results of the numerical solution consist of four parameters. This is as follows:

a: Punch-layer contact distance

b: Layer-quarter plane contact distance

P1max: Maximum stresses along the punch-layer contact distance

P2max: Maximum stresses along the layer-quarter plane contact distance.

#### *3.2.1 Contact stresses*

The change of maximum stress along the punch-layer contact distance with quarter plane gap distance and the change of maximum stress along the layer-quarter plane contact distance with quarter plane gap distance are shown in Fig. 6. As can be seen from the figure, the lowest values in stresses occurring both along the punch-layer distance and layer-quarter plane contact distance were obtained in the structure formed with the material properties obtained after the FSP application in P3 parameters. The main reason for this situation is the high strength and elongation values achieved in the material properties in this case. Thanks to the higher elongation values, the load is spread over a wider area during deformation, and thus the stress intensity decreases and the maximum stress values decrease. On the other hand, it is seen that the maximum stresses occurring along the layer-quarter plane distance increase with the

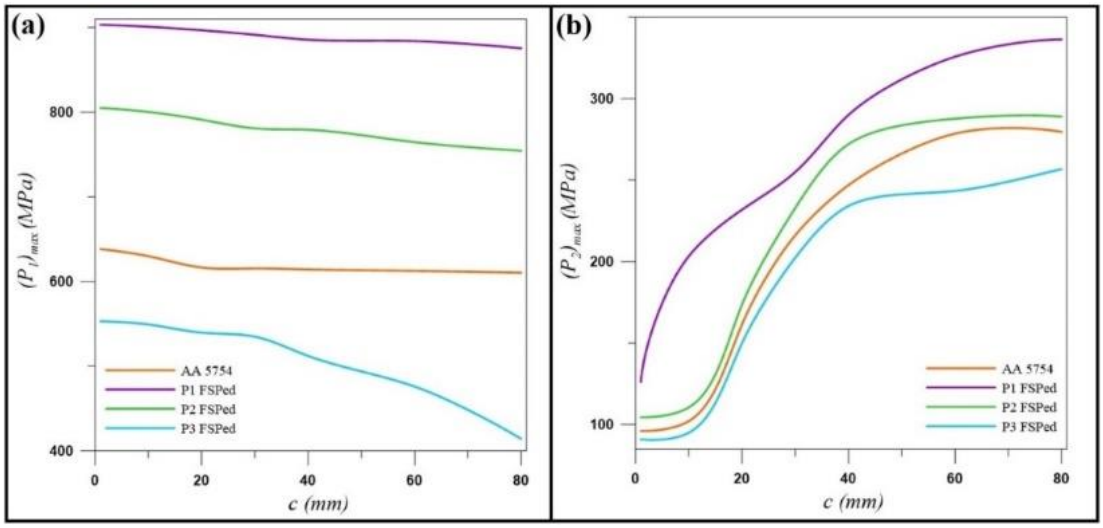


Fig. 6 (a) Variation of maximum stress along the punch-layer contact distance with quarter plane spacing distance and (b) variation of maximum stress along layer-quarter plane contact distance with quarter plane spacing distance

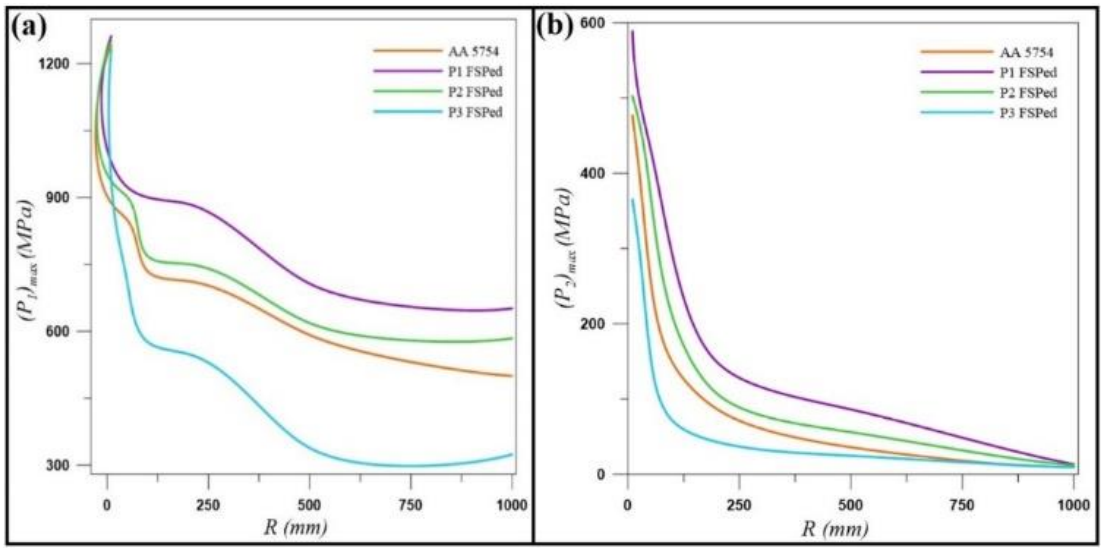


Fig. 7 (a) Variation of maximum stresses along the punch-layer contact distance with the circular punch radius, and (b) variation of maximum stress along the layer-quarter plane contact distance with the circular punch radius

increase in quarter plane distance in all cases. The reason for this situation is the decrease in the load-carrying area and the increase in stress intensity due to the increased quarter-plane gap distance.

The change of maximum stresses along the punch-layer contact distance and layer-quarter plane contact distance with the circular punch radius is shown in Fig. 7. It is seen that the maximum stresses occurring both along the punch-layer distance and along the layer-quarter plane distance decrease with the increase in the elongation properties of the materials (easier shaping). The main reason for this situation is that the load is spread over a wider area during deformation due to the easier shaping of the materials, resulting in decreased stress values due to the increased area. On the other hand, the maximum stresses occurring decrease with the increase in the punch radius for all cases. As it is known, as the sinking punch diameter increases, the stress intensity in the contact area decreases, and the maximum stresses decrease since the load is spread over a wider area. In parallel with this, the maximum stresses decrease with the increasing punch diameter for all conditions.

The change of maximum stresses along the punch-layer contact distance and layer-quarter plane contact distance with external load (P) is seen in Fig. 8. As can be seen, the lowest maximum stresses along both the punch-layer contact distance and layer-quarter plane contact distance were obtained when we modeled the model with the material to which we applied FSP in P3 parameters. The model with these material properties exhibits greater resistance to deformation and improved energy absorption capacity under loading. As a result, the model experiences lower maximum stresses. Conversely, as the external load increases, the contact area expands, distributing the load over a larger region. Therefore, the maximum stresses decrease with increasing external load in all cases.

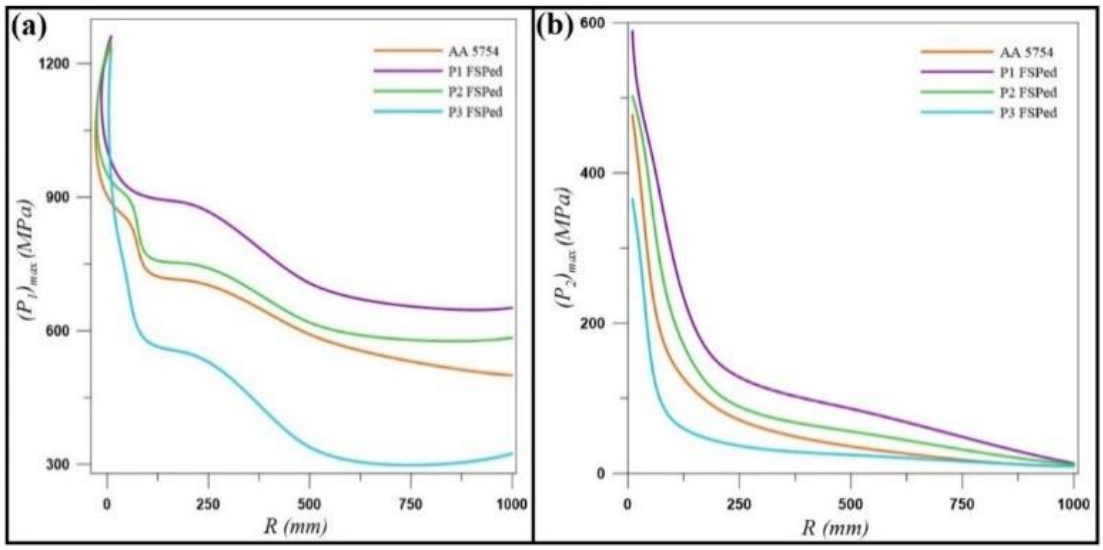


Fig. 8 (a) Variation of maximum stresses along the punch-layer contact distance with the circular external load, and (b) variation of maximum stress along the layer-quarter plane contact distance with the circular external load

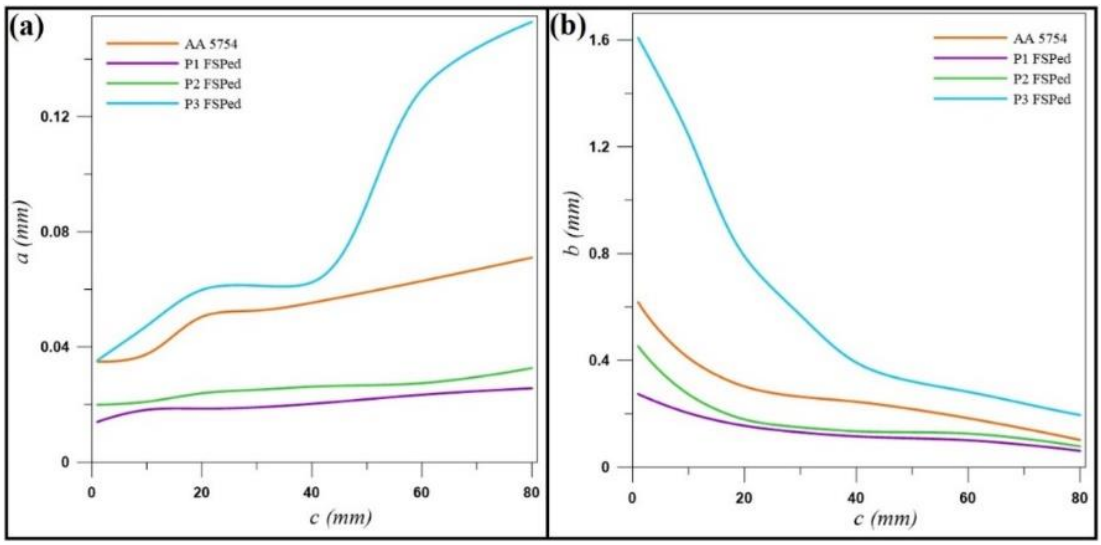


Fig. 9 (a) Variation of punch-layer contact distance with quarter plane clearance distance, and (b) variation of layer-quarter plane contact distance with quarter plane clearance distance

Additionally, since increased plastic deformation prevents localized stress concentrations, the maximum stress levels decline.

### *3.2.2 Contact distances*

The change of punch-layer contact distance and layer-quarter plane contact distance with quarter plane clearance distance is seen in Fig. 9. As a result of FEM analysis, it is seen that the highest punch-layer contact distance and layer-quarter plane contact distances are obtained in the case where the model is created with the material to which FSP is applied in the P3 parameter. The reason for this situation is that the P3 FSPed material has a higher elastic and plastic deformation capacity under load due to its high strength and ductility. In this way, the contact area expands, and both the punch-layer and layer-quarter plane contact distances increase compared to the cases modeled with other materials. On the other hand, when Fig. 9 is examined, it is seen that the punch-layer contact distance increases in all cases as the quarter plane clearance distance increases. The reason for this situation is that the load spreads to a wider area along the layer as the clearance distance increases. On the other hand, it was determined that the layer-quarter plane contact distance decreases with the increase in the quarter plane clearance distance for the cases modeled with all material properties. The reason for this is that the deformation in the part of the layer that touches the quarter plane decreases as the clearance distance increases.

The changes in the punch-layer contact distance and layer-quarter plane contact distance with the circular punch radius are shown in Fig. 10. As can be seen from the figure, both the highest punch-layer and the highest layer-quarter plane contact distances were obtained when the model was modeled with the material to which FSP was applied in the P3 parameter. The reason for this is the increase in the contact area resulting from the higher deformation under

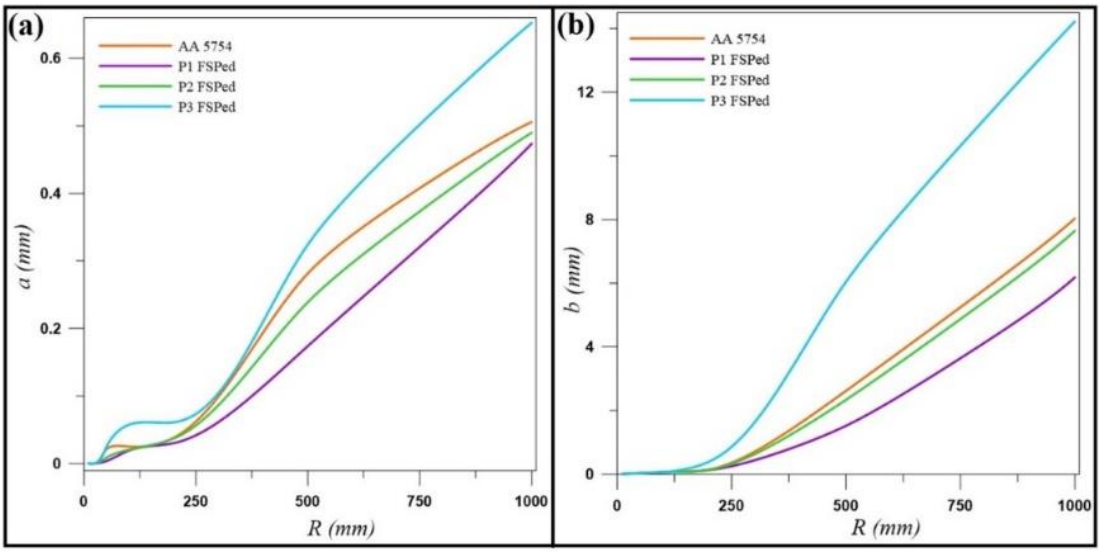


Fig. 10 (a) Variation of punch-layer contact distance with circular punch radius and (b) variation of layer-quarter plane contact distance with circular punch radius

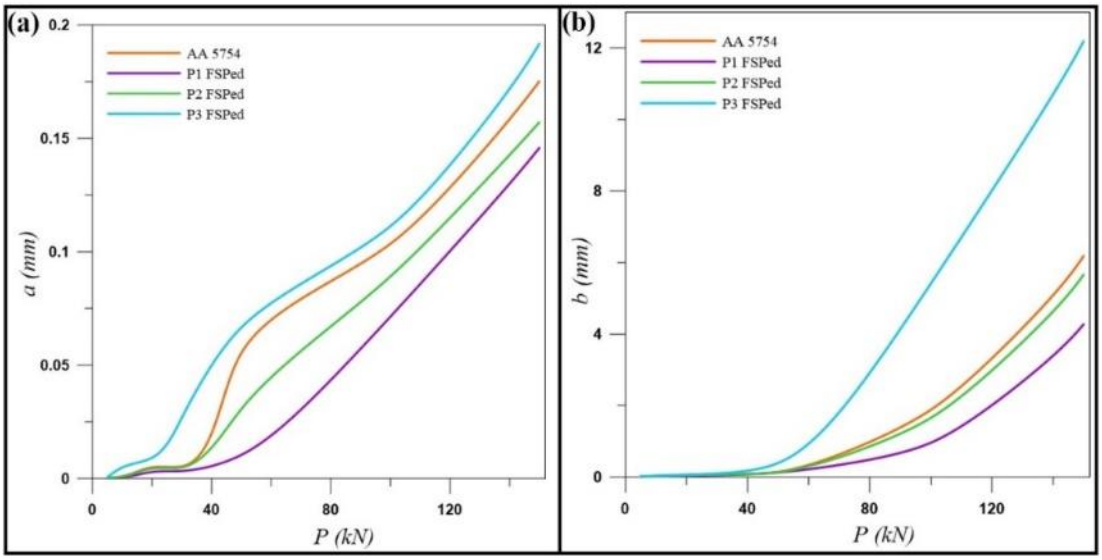


Fig. 11 (a) Variation of punch-layer contact distance with external load and (b) variation of layer-quarter plane contact distance with external load

load, which is a direct consequence of the high strength and ductility obtained in this parameter. Due to the high strength and elongation of this material, the load is distributed more homogeneously as the circular punch radius increases, and the contact distances increase compared to other conditions. On the other hand, the reason for the increase in distances with the increase in the circular punch radius in all cases is that the spread of the load over a wider area increases the deformation and causes the distances to grow.

The changes in the punch-layer contact distance and layer-quarter plane contact distance with external load (P) are shown in Fig. 11. As can be seen, the highest values in both the punch-layer and layer-quarter plane distances were obtained in the model created with the material properties obtained by applying FSP in the P3 parameter. The reason for this situation is that the structure modeled with this material allows more deformation under load, thanks to its high strength and ductility, which increases the contact areas. On the other hand, as the applied external load (P) increases, the punch-layer and layer-quarter plane contact distances increase because the increasing load causes more deformation on the material and expands the contact areas. These findings show that FSP-induced improvements in strength and ductility can greatly improve contact compliance and load distribution, which is crucial for reducing localized damage in contact-based mechanical systems.

In the study, FEM results were examined using variance analysis (ANOVA) for contact distances as shown in Fig. 12. The contour plots were created using MINITAB 19 software. While one value is fixed, the effect of the other two variables can be shown (Uzun Yaylacı 2022, Yaylacı *et al.* 2024). The changes in the punch-layer contact distance (a) according to external load (P), circular punch radius (R),

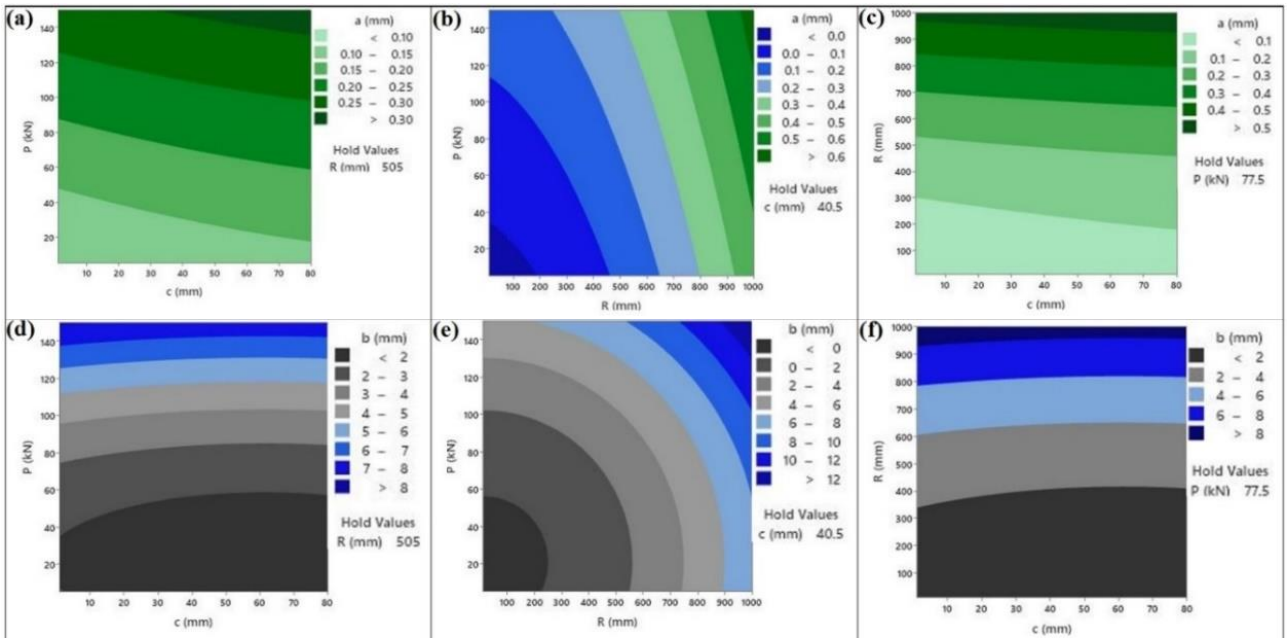


Fig. 11 (a) Variation of punch-layer contact distance with external load and (b) variation of layer-quarter plane contact distance with external load

and quarter plane spacing distance (c) are summarized in Fig. 12 (a-b-c). As can be seen, there is an increase in the punch-layer contact distance values for each case where the other two values, except for the value kept constant, are changed. On the other hand, the changes in the layer-quarter plane contact distance (b) values with variables are shown in Fig. 12 (d-e-f). As can be seen, when the R variable is kept constant, the increase in the P value is more effective in increasing the layer-quarter plane contact distances. Similarly, when the P value was kept constant, the increasing R value was more effective increasing the layer-quarter plane contact distance. It can be seen from the figure that the increase in both P and R values created an increasing effect on the layer-quarter plane contact distance at the fixed c value.

## 4. Conclusions

In this work, FSP was applied to Al 5754 alloy under three different settings, and the changes in the material's strength and elongation values after FSP were compared to the situation before the FSP. In the following step of the investigation, the changing strength and elongation values were translated to finite element (FEM) analyses to determine the impact these changes had on the contact stresses and distance values of the structures in contact. The data obtained as a result of the study are summarized below:

1- After all the FSPs were made after changing the parameters, the yield and tensile strengths increased compared to the base material. The highest yield and tensile strengths were reached after the FSP was made in the P3 coded parameter with the values of 291 MPa and 378 MPa, respectively.

2- The elongation values of the main material decreased after the FSP made in the P1 and P2 coded parameters and increased after the P3 coded FSP.

3- In the modeled contact problem, the contact stresses obtained in the system exhibited a decreasing trend with the increase in material strength and elongation in all the different input parameters, such as external load, circular punch radius, and quarter plane spacing distance.

4- In the contact system, the contact distances increased with increasing strength and elongation values in all the input parameters that were changed.

As can be seen, the increases experienced together in the strength and elongation of the materials used in the contact structures lead to improvements in terms of contact stresses and distances. On the other hand, the study has observed that the changes experienced in the strength and elongation of the materials after FSP can change sharply with the FSP parameters used. In this context, using the strength and elongation values of the materials in contact systems by improving them without experiencing changes in their chemical composition can be considered as an optimum solution. Also, the study reveals that the correct selection of the parameters to be applied during FSP is highly critical in the mechanics of the contact systems.

## References

Abrahams, R., Mikhail, J. and Fasihi, P. (2019), "Effect of friction stir process parameters on the mechanical properties of 5005-H34 and 7075-T651 aluminium alloys", *Mater. Sci. Eng. A*, **751**, 363-373. https://doi.org/10.1016/j.msea.2019.02.065.

Aktarer, S.M., Küçükömeroğlu, T. and Davut, K. (2019), "Friction stir processing of dual phase steel: Microstructural evolution and mechanical properties", *Mater. Charact.*, **155**, 109787. https://doi.org/10.1016/j.matchar.2019.109787.

Aktarer, S.M., Sekban, D.M., Yanar, H. and Purçek, G. (2017), "Effect of friction stir processing on tribological properties of Al-Si alloys", *IOP Conference Series: Materials Science and*

*Engineering*, **174**(1), 012061. https://doi.org/10.1088/1757-899X/174/1/012061.

Ammarullah, M.I., Kozin, M., Maula, M.I., Danny Pratama Lamura, M., Wicaksono, H.A., Bayuseno, A.P., Jamari J. and Ramlee, M.H. (2025), "A review of enhanced total hip prosthesis design and material bearing combination to accommodate Muslim prayer (Salat) movements: Biomechanical, biotribological, and biological perspectives", *Tribol. Int.*, **205**, 110518. https://doi.org/10.1016/j.triboint.2025.110518.

Ammarullah, M.I. (2025), "Integrating finite element analysis in total hip arthroplasty for childhood hip disorders: Enhancing precision and outcomes", *World J. Orthop.*, **16**(1), 98871. https://doi.org/10.5312/wjo.v16.i1.98871.

Benouis, A., Zagane, M.E.S., Moulgada, A., Yaylacı, M., Ait kaci, D., Terzi, M., Özdemir, M.E. and Uzun Yaylacı, E. (2024), "Finite element analysis of the behavior of elliptical cracks emanating from the orthopedic cement interface in total hip prostheses", *Struct. Eng. Mech.*, **89**(5), 539-547. https://doi.org/10.12989/sem.2024.89.8.539.

Chaudhary, A., Kumar Dev, A., Goel, A., Butola, R. and Ranganath, M.S. (2018), "The mechanical properties of different alloys in friction stir processing: A Review", *Mater. Today: Proc.*, **5**(2-1), 5553-5562. https://doi.org/10.1016/j.matpr.2017.12.146.

Das, S., Heyen, M., Ho, J. and Son, C. (2020), "Effect of processing parameters on the formability of recycle friendly AA5754 alloy", *MATEC Web of Conferences*, **326**, 03005. https://doi.org/10.1051/matecconf/202032603005.

El-Ashmawy, A.M. and Xu, Y. (2022), "An efficient C 1 beam element via multi-scale material adaptable shape function", *Adv. Nano Res.*, **13**(4), 351-368. https://doi.org/10.12989/anr.2022.13.4.351.

El-Sayed, M.S., Ibrahim, M. and Abdel-Aziz, A.I. (2025), "Effect of friction stir processing parameters on mechanical properties of different aluminum alloy plates", *Sci. Rep.*, **15**(1), 27066. https://doi.org/10.1038/s41598-025-11948-1.

Fu, J., Haeri, H., Sarfarazi, V., Khodakaram Zadeh, R., Amini, E., Amini, M.S. and Karimi, L. (2025a), "Computational and experimental analysis of failure characteristics in geogrid-reinforced pre-holed subsurface materials", *Eng. Fract. Mech.*, **315**, 110857. https://doi.org/10.1016/j.engfracmech.2025.110857.

Fu, J., Haeri, H., Sarfarazi, V., Rafiei, N., Amiri, A.A. and Marji, M.F. (2025b), "Investigation of the shear mechanism at the interface between grout and brittle rock: physical testing and PFC3D simulation", *Int. J. Numer. Anal. Methods Geomech.*, **49**(5), 1491-1505. https://doi.org/10.1002/nag.3944.

Fuyad, S.T.M., Al Bari, M.A., Makfidunnabi, M., Nain, H.Z., Özdemir, M.E. and Yaylacı, M. (2024), "Finite element analysis of ratcheting on beam under bending-bending loading conditions", *Struct. Eng. Mech.*, **89**(1), 023. https://doi.org/10.12989/sem.2024.89.1.023.

Ghaednia, H., Wang, X., Saha, S., Xu, Y., Sharma, A. and Jackson, R.L. (2017), "A Review of Elastic–Plastic Contact Mechanics", *Appl. Mech. Rev.*, **69**(6), 060804. https://doi.org/10.1115/1.4038187.

Guru, P.R., Khan Md, F., Panigrahi, S.K. and Ram, G.D.J. (2015), "Enhancing strength, ductility and machinability of a Al–Si cast alloy by friction stir processing", *J. Manuf. Process.*, **18**, 67-74. https://doi.org/10.1016/j.jmapro.2015.01.005.

Güvercin, Y., Yaylacı, M., Dizdar, A., Özdemir, M.E., Ay, S., Yaylacı, E.U., Karahasanoğlu, U., Uygun, H. and Peker, G. (2025), "Biomechanical analysis and solution suggestions of screw replacement scenarios in femoral neck fracture surgeries: Finite element method", *Orthop. Surg.*, **17**, 614-623. https://doi.org/10.1111/os.14337.

Haeri, H. and Sarfarazi, V. (2016), "The deformable multilaminate for predicting the elasto-plastic behavior of rocks", *Comput. Concr.*, **18**(2), 201-214. https://doi.org/10.12989/cac.2016.18.2.201.

Hidayat, T., Ammarullah, M.I., Ismail, R., Tauviqirrahman, M., Saputra, E., Lamura, M.D.P., Chethan, K.N., Bayuseno, A.P. and Jamari J. (2024), "Assessment of polyethylene wear in dual mobility implant for Asians on various head-to-liner ratios: A finite-element analysis", *Proc. Inst. Mech. Eng. J: J. Eng. Tribol.*, **238**(8), 943-955. https://doi.org/10.1177/13506501241240021.

Karthikeyan, L. and Senthil Kumar, V.S. (2011), "Relationship between process parameters and mechanical properties of friction stir processed AA6063-T6 aluminum alloy", *Mater. Des.*, **32**(5), 3085-3091. https://doi.org/10.1016/j.matdes.2010.12.049.

Khodabakhshi, F., Gerlich, A.P. and Švec, P. (2017), "Fabrication of a high strength ultra-fine grained Al-Mg-SiC nanocomposite by multi-step friction-stir processing", *Mater. Sci. Eng. A*, **698**, 313-325. https://doi.org/10.1016/j.msea.2017.05.065.

Kiarasi, F., Babaei, M., Mollaei, S., Mohammadi, M. and Asemi, K. (2021), "Free vibration analysis of FG porous joined truncated conical-cylindrical shell reinforced by graphene platelets", *Adv. Nano Res.*, **11**(4), 361-380. https://doi.org/10.12989/anr.2021.11.4.361.

Kumar, A., Pal, K. and Mula, S. (2017), "Simultaneous improvement of mechanical strength, ductility and corrosion resistance of stir cast Al7075-2% SiC micro- and nanocomposites by friction stir processing", *J. Manuf. Process.*, **30**, 1-13. https://doi.org/10.1016/j.jmapro.2017.09.005.

Lamura, M.D.P., Ammarullah, M.I., Maula, M.I., Hidayat, T., Bayuseno, A.P. and Jamari, J. (2024), "The effect of load, diameter ratio, and friction coefficient on residual stress in a hemispherical contact for application in biomedical industry", *J. Mater. Eng. Perform.*, **33**(15), 7528-7536. https://doi.org/10.1007/s11665-024-09330-9.

Leal, R.M., Galvão, I., Loureiro, A. and Rodrigues, D.M. (2015), "Effect of friction stir processing parameters on the microstructural and electrical properties of copper", *Int. J. Adv. Manuf. Technol.*, **80**(9), 1655-1663. https://doi.org/10.1007/s00170-015-7141-z.

Mishra, R.S., De, P.S. and Kumar, N. (2014), *Friction Stir Processing*, In *Friction Stir Welding and Processing: Science and Engineering*, 259-296, Cham: Springer International Publishing.

Moulgada, A., Zagane M.E.S., Yaylacı, M., Ait Kaci, D., Benouis, A., Baltach, A., Öztürk, Ş., Özdemir, M.E. and Uzun Yaylacı, E. (2024), Effects of the stiffness of an inclusion on the mechanical behavior of an aluminum alloy plate with a lateral notch", *Steel Compos. Struct.*, **51**(1), 63-72. https://doi.org/0.12989/scs.2024.51.1.063.

Muchammad, M., Tauviqirrahman, M., Ammarullah, M.I., Iqbal, M., Setiyana, B. and Jamari, J. (2024), "Performance of textured dual mobility total hip prosthesis with a concave dimple during Muslim prayer movements", *Sci. Rep.*, **14**(1), 916. https://doi.org/10.1038/s41598-023-50887-7.

Murugesan, R., Venkataraman, S.H., Sahoo, P.K., Anand, P.B., Rithick, R. and Ammarullah, M.I. (2025), "Fatigue analysis and load spectrum generation for wing-fuselage lug joint with a focus on human safety transport category aircraft", *Eng. Rep.*, **7**(3), e70053. https://doi.org/10.1002/eng2.70053.

Naumov, A.A., Safi, S.V. and Safi, S.M. (2025), "Advances in friction stir processing of aluminum 2024: A review of nanoparticle-reinforced surface composites", *Int. J. Adv. Manuf. Technol.*, **137**(7), 3141-3164. https://doi.org/10.1007/s00170-025-15332-1.

Öner, E. (2021a), "Frictionless contact mechanics of an orthotropic coating/isotropic substrate system", *Comput. Concr.*, **28**, 209-

220. https://doi.org/10.12989/cac.2021.28.2.209.
Öner, E. (2021b), "Two-dimensional frictionless contact analysis of an orthotropic layer under gravity", *J. Mech. Mater. Struct.*, **16**, 573-594. https://doi.org/10.2140/jomms.2021.16.573.
Öner, E. and Birinci, A. (2014), "Continuous contact problem for two elastic layers resting on an elastic half-infinite plane", *J. Mech. Mater. Struct.*, **9**, 105-119. https://doi.org/10.2140/jomms.2014.9.105.
Öner, E. and Birinci, A. (2020), "Investigation of the solution for discontinuous contact problem between a functionally graded (FG) layer and homogeneous half-space", *Arch. Appl. Mech.*, **90**, 2799-2819. https://doi.org/10.1007/s00419-020-01750-y.
Öner, E., Oktay, M.G., Uzun Yaylacı, E., Yaylacı, M. and Mirzaloğlu, İ. (2025), "Tri-method analysis of contact mechanics in orthotropic-isotropic materials", *Arch. Appl. Mech.*, **95**, 116. https://doi.org/10.1007/s00419-025-02832-5.
Padhy, G.K., Wu, C.S. and Gao, S. (2018), "Friction stir based welding and processing technologies - processes, parameters, microstructures and applications: A review", *J. Mater. Sci. Technol.*, **34**(1), 1-38. https://doi.org/10.1016/j.jmst.2017.11.029.
Pointner, P. (2008), "High strength rail steels—The importance of material properties in contact mechanics problems", *Wear*, **265**(9), 1373-1379. https://doi.org/10.1016/j.wear.2008.03.015.
Sarfarazi, V., Haeri, H. and Shemirani, A.B. (2017), "Direct and indirect methods for determination of mode I fracture toughness using PFC2D", *Comput. Concr.*, **20**(1), 39-47. https://doi.org/10.12989/cac.2017.20.1.039.
Sekban, D.M. (2024), "Effect of friction stir process on mechanical properties and bottom section ultimate strength of ship steel", *J. Mater. Eng. Perform.*, **34**, 9772-9780. https://doi.org/10.1007/s11665-024-09791-y.
Sekban, D.M., Saray, O., Aktarer, S.M., Purcek, G. and Ma, Z.Y. (2015), "Microstructure, mechanical properties and formability of friction stir processed interstitial-free steel", *Mater. Sci. Eng. A*, **642**, 57-64. https://doi.org/10.1016/j.msea.2015.06.068.
Sekban, D.M., Uzun Yaylacı, E., Özdemir, M.E. and Yaylacı, M. (2024b), "Determination of formability behavior of steel used in ships by various methods", *Struct. Eng. Mech.*, **92**(2), 189-196. https://doi.org/10.12989/sem.2024.92.2.189.
Sekban, D.M., Uzun Yaylacı, E., Özdemir, M.E., Öztürk, Ş., Yaylacı, M. and Panda, S.K. (2024a), "Formability behavior of AH-32 shipbuilding steel strengthened by friction stir process", *Theor. Appl. Fract. Mec.*, **132**, 104485. https://doi.org/10.1016/j.tafmec.2024.104485.
Selvamani, R., Ebrahimi, F., Yaylacı, M., Öztürk, Ş. and Uzun Yaylacı, E. (2024), "Nonlinear poro-thermo-forced vibration in curved sandwich magneto-electro-elastic shells under hygrothermal environment", *Acta. Mech.*, **235**, 5489-5528. https://doi.org/10.1007/s00707-024-03994-z.
Serio, L.M., Palumbo, D., De Filippis, L.A.C., Galietti, U. and Ludovico, A.D. (2016), "Effect of friction stir process parameters on the mechanical and thermal behavior of 5754-H111 aluminum plates", *Materials*, **9**(3), 122. https://doi.org/10.3390/ma9030122.
Singh, P., Sahai, A. and Sharma, R.S. (2023), "Insights into the friction stir processing of fused filament fabricated polymers with multiple reinforcements", *Polym-Plast. Tech. Mat.*, **62**(12), 1621-1638. https://doi.org/10.1080/25740881.2023.2227246.
Singh, S., Kaur, M. and Saravanan, I. (2020), "Enhanced microstructure and mechanical properties of boiler steel via Friction Stir Processing", *Mater. Today: Proc.*, **22**, 482-486. https://doi.org/10.1016/j.matpr.2019.07.724.
Starink, M.J., Deschamps, A. and Wang, S.C. (2008), "The strength of friction stir welded and friction stir processed aluminium alloys", *Scripta Materialia*, **58**(5), 377-382. https://doi.org/10.1016/j.scriptamat.2007.09.061.
Sun, N., Jones, W.J. and Apelian, D. (2019), "Friction Stir Processing of Aluminum Alloy A206: Part II—Tensile and Fatigue Properties", *Int. J. Metalcast.*, **13**(2), 244-254. https://doi.org/10.1007/s40962-018-0268-6.
Surekha, K. and Els-Botes, A. (2011), "Development of high strength, high conductivity copper by friction stir processing", *Mater. Des.*, **32**(2), 911-916. https://doi.org/10.1016/j.matdes.2010.08.028.
Surekha, K., Murty, B.S. and Prasad Rao, K. (2009), "Effect of processing parameters on the corrosion behaviour of friction stir processed AA 2219 aluminum alloy", *Solid State Sci.*, **11**(4), 907-917. https://doi.org/10.1016/j.solidstatesciences.2008.11.007.
Tauviqirrahman, M., Lim, Y., Jamari, J., Muchammad, M., Pugastri, B.O., Yohana, E. and Ammarullah, M.I. (2024), "A comparative study on turbulent models for three-dimensional thermo-hydrodynamic analysis of textured thrust bearing", *Cogent Eng.*, **11**(1), 2402048. https://doi.org/10.1080/23311916.2024.2402048.
Tosun, G., Ozler, L. and Ozcan, M.E. (2020), "Gradient composite coatings on AA5754 using friction stir process", *Surf. Eng.*, **36**(5), 447-455. https://doi.org/10.1080/02670844.2019.1665279.
Turan, M., Kahya, V., Uzun Yaylacı, E. and Yaylacı, M. (2025), "A shear deformable numerical approaches for the static analysis of bi-directional functionally graded beams", *Adv. Nano Res.*, **18**(2), 143-162. https://doi.org/10.12989/anr.2025.18.2.143.
Uzun YayIacı, E. (2022), "Characterization of Pseudoalteromonas sp. from aquaculture environment and optimization of fermentation culture parameters by RSM-Based modeling", *Turk. J. Fish. Aquat. Sci.*, **22**(11). https://doi.org/10.4194/TRJFAS21726.
Vaira Vignesh, R. and Padmanaban, R. (2018), "Influence of friction stir processing parameters on the wear resistance of aluminium alloy AA5083", *Mater. Today: Proc.*, **5**(2-2), 7437-7446. https://doi.org/10.1016/j.matpr.2017.11.415.
Wang, J.T., Liu, A.X., Zhang, Y.K., Xie, L., He, M.T., Luo, K.Y. and Hu, K.J. (2025), "Influence of process parameters on wear resistance of surfaces modified by friction stirring processing in 7075 Aluminum alloy", *Met. Mater. Int.*, **31**(3), 625-635. https://doi.org/10.1007/s12540-024-01783-w.
Wang, W., Han, P., Peng, P., Zhang, T., Liu, Q., Yuan, S.N., Huang, L.Y., Yu, H.L., Qiao, K. and Wang, K.S. (2020), "Friction stir processing of magnesium alloys: A Review", *Acta Metall. Sin.*, **33**(1), 43-57. https://doi.org/10.1007/s40195-019-00971-7.
Wang, X., Guo, X., Babaei, M., Fili, R. and Farahani, H. (2023), "Natural frequency analysis of joined conical-cylindrical-conical shells made of graphene platelet reinforced composite resting on Winkler elastic foundation", *Adv. Nano Res.*, **15**(4), 367-384. https://doi.org/10.12989/anr.2023.15.4.367.
Wu, X. (2023), "Nonlinear finite element vibration analysis of functionally graded nanocomposite spherical shells reinforced with graphene platelets", *Adv. Nano Res.*, **15**(2), 141-153. https://doi.org/10.12989/anr.2023.15.2.141.
Yadav, D. and Bauri, R. (2012), "Effect of friction stir processing on microstructure and mechanical properties of aluminium", *Mater. Sci. Eng. A*, **539**, 85-92. https://doi.org/10.1016/j.msea.2012.01.055.
Yang, Y., Zuo, W., Liu, Y., Ge, Y., Yang, Z., Han, J. and Mi, Z. (2024), "Fabrication of medium Mn advanced high-strength steel with excellent mechanical properties by friction stir processing", *Micromachines*, **15**(8), 1052. https://doi.org/10.3390/mi15081052.
Yaylacı, M., Öner, E., Adıyaman, G., Öztürk, Ş., Uzun Yaylacı, E. and Birinci, A. (2024), "Analyzing of continuous and discontinuous contact problems of a functionally graded layer: theory of elasticity and finite element method", *Mech. Based*

*Des. Struct. Mach.*, **52**(8), 5720-5738. https://doi.org/10.1080/15397734.2023.2262562.

Yaylacı, M., Yazıcıoğlu, A., Uzun Yaylacı, E., Terzi, M. and Birinci, A. (2025), "Evaluation of the contact problem of two layers one of functionally graded, loaded by circular rigid block and resting on a Pasternak foundation by analytical and numerical (FEM and MLP) methods", *Arch. Appl. Mech.*, **95**, 78. https://doi.org/10.1007/s00419-025-02787-7.

Yemenoglu, H., Beder, M., Yaylacı, M., Dizdar, A., Alkurt, M., Naralan, M.E., Uzun Yaylacı, E., Özdemir, M.E., Öztürk, Ş. and Yeşil, Z. (2025), "Evaluation of prostheses retained zygomatic and dental implants in large defects in the maxilla due to tumors or major trauma by biomechanical 3- 3-dimensional finite element analysis", *BMC Oral Health*, **25**(1), 99. https://doi.org/10.1186/s12903-025-05468-7.

Zhao, H., Pan, Q., Qin, Q., Wu, Y. and Su, X. (2019), "Effect of the processing parameters of friction stir processing on the microstructure and mechanical properties of 6063 aluminum alloy", *Mater. Sci. Eng. A*, **751**, 70-79. https://doi.org/10.1016/j.msea.2019.02.064.

Zheng, Y., Jin, H. and Jiang, C. (2022), "Assessment of nonlinear stability of geometrically imperfect nanoparticle-reinforced beam based on numerical method", *Adv. Nano Res.*, **13**(2), 113-120. https://doi.org/10.12989/anr.2022.13.2.113.

*CC*